SCIENCE CHINA
Chemistry

• ARTICLES •

June 2014 Vol.57 No.6: 842–848
doi: 10.1007/s11426-014-5088-9

Urease inactivation by an unusual GroES chaperonin

CUN ShuJian[1,2] & SUN HongZhe[1*]

[1]*Department of Chemistry, The University of Hong Kong, Hong Kong, China*
[2]*Department of Chemistry, The Scripps Research Institute, La Jolla CA 92037, USA*

Received November 20, 2013; accepted February 10, 2014; published online February 21, 2014

It remains uncovered yet how the common gastric pathogen, *Helicobacter pylori*, survives through the acidic barrier and the immune response simultaneously in the stomach. Herein we report a unique GroES chaperonin that effectively inactivates *Helicobacter pylori* urease in *Escherichia coli* model. Such a function depends on the quaternary structure as well as the metal binding at the C terminus. Surprisingly, the C-terminal metal capacity seems not closely relevant to the apparent urease inactivation. Our findings have possibly revealed a survival strategy of *Helicobacter pylori* after its gastric localization.

GroES chaperonin, *Helicobacter pylori*, metal binding, microbial pathogenesis, nickel, urease inactivation

1 Introduction

As the major cause of gastric diseases [1], *Helicobacter pylori* (*H. pylori*), successfully overcomes two difficult challenges to infect over half of the world population. The first is the extremely acidic fluid in the gastric lumen that can demolish most life forms. Being a neutrophilic Gram-negative bacterium, *H. pylori* heavily relies on the nickel-containing enzyme, urease [2], to catalyze the hydrolysis of urea into ammonia and carbonate, and thus maintains pH homeostasis in excess protons [3]. The second challenge comes from the immune system of mammalian hosts. After migrating from the acidic lumen to the neutral epithelial layer, *H. pylori* needs to deal with antimicrobial nitric oxide (NO) that is produced by inducible nitric oxide synthase (iNOS) due to immune response. To resist the lethal chemical, the bacterium utilizes arginase to compete the substrate with iNOS, consequently resulting in the generation of L-ornithine and urea instead of NO [4].

However, such strategies could also lead *H. pylori* to a survival dilemma: being a neutrophilic bacterium, *H. pylori* has been found to be susceptible to urea hydrolysis when cultivated in a neutral medium [5], suggesting that its survival does not only require the urease to be active under acidic conditions, but also inactive at neutral pH in the presence of urea. In spite of enormous efforts devoted to the study on the activation of urease, which is delicately assisted by a battery of chaperonins [6], it is still unknown whether and how the enzyme is inactivated to date.

In general, an unusual sequence of a protein usually implies an unusual origin in the evolution, and more importantly, an unusual evolutionary origin is frequently connected to an unusual survival strategy. Therefore, it looks fascinating whether *H. pylori* manages to conquer the extreme acidity as well as the immune attack with assistance from any alien component, such as its unique GroES chaperonin. After all, the roles of chaperones in pathogenesis have been suggested for a long time [7]. Being a ubiquitously studied chaperone system, GroEL/S non-specifically recognizes and refolds non-native proteins [8]. Meanwhile, both GroES and GroEL remain highly conserved throughout life kingdoms [9]. Consequently, the rich functionality of this system is one of its greatest strengths, providing an evolving potency that may adapt new functions via minor modification. GroES is conventionally regarded as a co-chaperonin that assists GroEL to fulfil chaperone functions [10]. In *H. pylori*, the GroEL chaperonin (*Hp*GroEL, also

*Corresponding author (email: hsun@hku.hk)

named as the heat-shock protein B, HspB) exhibits little variance among the family members [11]. Nevertheless, the bacterium employs a unique version of GroES (*Hp*GroES, also known as the heat-shock protein A, HspA), which possesses a rare histidine/cysteine-rich domain at the C-terminus, probably serving as a metal-binding domain (MBD) [12, 13].

2 Materials and methods

2.1 Construction of expression vectors

The *groES* genes were amplified from *H. pylori* strain 26695 and *E. coli* strain K-12. Endonuclease restriction sites were introduced to appropriate positions by QuickChange XL site-directed mutagenesis kit (Stratagene), and thus the coding sequences were recombined to produce the GroES derivatives.

2.2 Protein purification

For the MBD-deleted variants, the proteins were isolated in accordance with a previously established protocol [15]. For the proteins with the MBD, they were readily purified from the cell extracts using a nickel-NTA affinity column (Novagen) [13]. The identities of the purified proteins as well as the urease were confirmed by MALDI-TOF mass spectrometry (ABI4800 MALDI TOF/TOF™ Analyzer).

2.3 Prediction of terminal interfacial residues

The model of *Hp*GroES was retrieved from MODBASE [16] with the accession number P0A0R4. The computational structure was generated using the GroES structure of *Mycobacterium tuberculosis* (PDB ID: 1P3H) as a template, for its highest similarity to *Hp*GroES among the structure-determined homologs to date, leaving the structure of the MBD unresolved due to lacking of a template.

2.4 Determination of oligomeric states

Analytical size-exclusive gel filtration chromatography was performed on a Superdex 75 10/300 GL column (GE Healthcare) in 50 mM Tris-HCl (pH 7.5) and 100 mM NaCl. The low-molecular-weight gel filtration calibration kit (GE Healthcare) was used as the reference of molecular masses.

2.5 Co-expression of urease and GroES variants in *E. coli* cells

The gene cluster that encodes urease subunits (i.e. UreA and UreB) and a battery of maturation-assistant partners, including UreI, UreE, UreF, UreG, UreH and NixA, were translocated from *H. pylori* genomic DNA to chloramphenicol-resistant plasmid (termed as pHP8080) [17]. The ampicillin-resistant plasmids of GroES variants were constructed from pET-23 expression vector (EMD Millipore) with no extra tag. The two sets of plasmids were subsequently transformed into *E. coli* BL21 (DE3). Then the *E. coli* cells were grown in dual antibiotics of 100 μg/mL ampicillin and 25 μg/mL chloramphenicol. The proportions of the expressed proteins in the total were estimated by pixel quantification using ImageJ software [18] with digitized gel image of 15%-acrylamide SDS-PAGE.

2.6 Biochemical assays of urease activity

E. coli cells were cultivated in M9 minimal medium (Sigma-Aldrich) in the absence of Ni^{2+}. When OD_{600} = 1.0, nickel sulfate ($NiSO_4$) and IPTG were supplemented to final concentration of 1 μM and 0.1 mM, respectively. After 1-h incubation, the culturing media were refreshed with acidic minimal media (pH 5.0) containing 50 mM urea. The pH meter was calibrated with standard buffers prior to the measurement each time. Alternatively, the phenol-hypochlorite determination [17] was performed for urease assays, using the cell extracts that were released by sonication in 50 mM Hepes (pH 7.5) and 100 mM NaCl.

2.7 *In situ* visualization of active urease

Cell extracts from *H. pylori* or *E. coli* (as examined above) were subjected to native electrophoresis in 13% polyacrylamide gel, where similar amounts of total protein were loaded (as ensured by Bradford assay [19]). After electrophoresis, the gel was placed in Hepes buffer with pH indicator (i.e. 0.5% *w/v* phenol red) for 15 min to get equilibrated. Then 50 mM urea was added to the buffer and catalyzed into ammonia within seconds if in-gel urease was active. Due to local pH increase, active urease could thus be visualized *in situ*. The 8-bit digital image of the gel was analyzed by pixel quantification with NIH ImageJ software [18].

2.8 Estimation of nickel-binding capacity

The apo-*Hp*GroES-MBD_2 was titrated by 10 mM $NiSO_4$ in 50 mM Tris-HCl (pH 7.5), 100 mM NaCl, and the UV-Visible absorption at 316 nm (A_{316}) was used to monitor the Ni^{2+}-protein coordination as reported previously [13]. The goodness of fit was evaluated by R^2. The data were fitted to the one-site binding (hyperbola) formula if applicable.

3 Results

3.1 Sample preparation and selection of cell model

Both wild-type and mutant GroES proteins (see sequences

in Figure 1) were over-expressed and purified (Figure 2(a)) so as to examine their physiochemical properties, and also co-expressed with urease-related proteins in comparable expression levels (Figure 2(b)). In this study, the neutrophilic Gram-negative bacterium, *Escherichia coli* (*E. coli*), was chosen as a model system to simulate an environment where the interested biochemical effects can be investigated under control more strictly than in the native host (i.e. *H. pylori*).

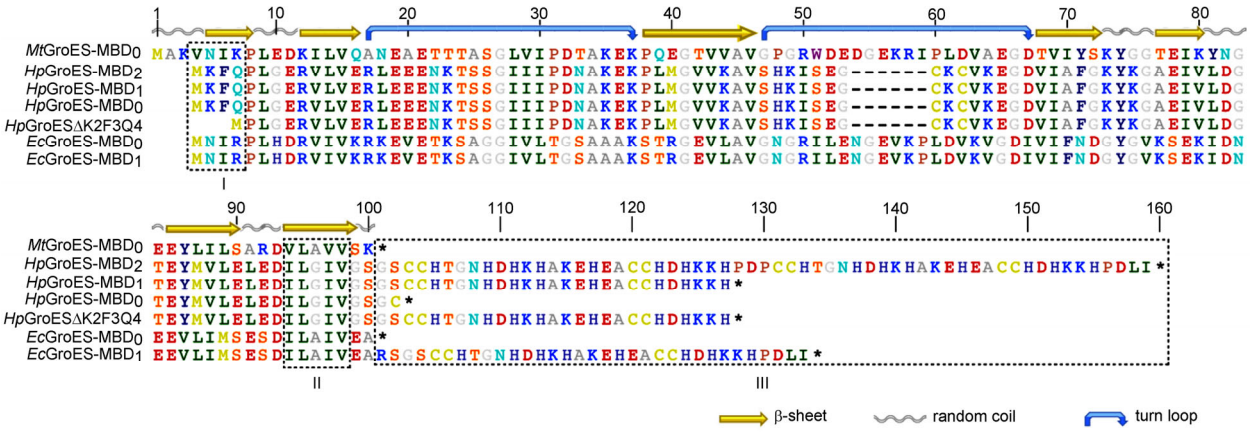

Figure 1 An overview of the proteins investigated in this work. Sequences were aligned by ClustalW program, and residues were colored in RasMol scheme. The secondary structure elements are indicated with reference to the structure of *Mt*GroES. The tentative interfacial residues are highlighted in box I for the N terminus and box II for the C terminus, respectively. The C termini with or without the MBD are marked in box III.

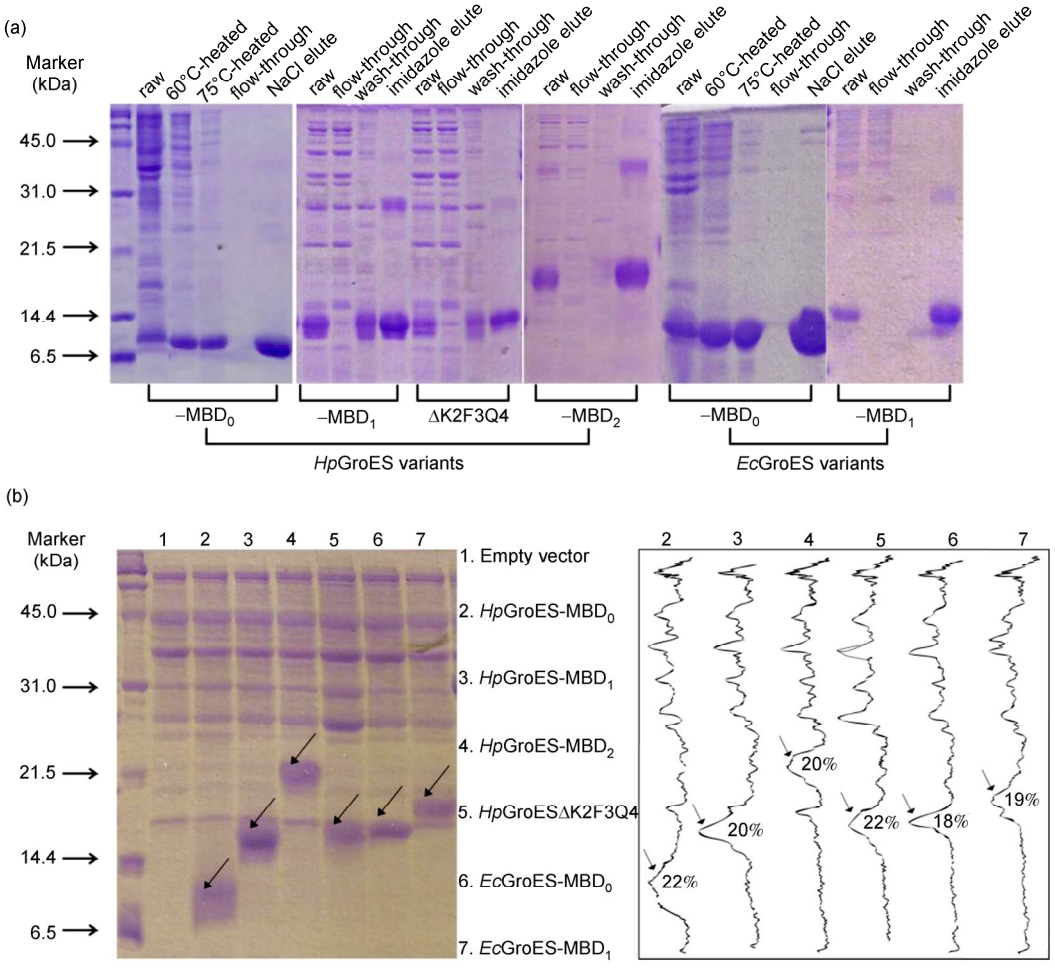

Figure 2 (a) Protein overexpression and purification of GroES mutants in this study. (b) Expression profiles of *E. coli* cells that host urease and *groES* genes. Protein contents were examined in 15% polyacrylamide gel by SDS-PAGE. Pixel densities of the digital gel image were converted into peak areas shown on the right side, so that the expressed proteins could be quantitatively evaluated.

3.2 The urease inactivation depends on the native heptameric structure of GroES

It has been reported that the complete function of GroES heavily relies on its heptameric quaternary structure [20]. With respect to the modeled structure, the C terminus of *Hp*GroES could be independent from the oligomeric interfaces (Figure 3), and therefore the length variation of this region should have little interference with the main structure. Indeed, when the *Hp*GroES mutant with duplicated MBD (*Hp*GroES-MBD_2) was purified and subjected to gel filtration chromatography, the elution volume was 9.2 mL under native conditions (Figure 4(a)), corresponding to a molecular mass of ~160 kDa that implicates a native oligomeric state as a heptamer referring to the theoretical size of a monomer (16.6 kDa). Under identical conditions, the wild-type *Hp*GroES (termed as *Hp*GroES-MBD_1) and the MBD-truncated *Hp*GroES (i.e. *Hp*GroES-MBD_0) eluted individually at 9.7 and 10.0 mL (Figure 4(b) and (c)), corresponding to the molecular masses of ~120 and ~100 kDa respectively. With the monomeric sizes as 13.0 and 10.1 kDa, the two proteins thus retained their native heptameric forms regardless of the varying length of the C terminus, indicating that the extension of the C terminus had no evident interference with the structural integrity under these conditions. Furthermore, recalling that the GroES heptamer is generally maintained through the hydrophobic interaction of the terminal residues [21], the terminal deletion may disrupt the interface of the quaternary structure. The residues Met1 and Phe3 at the N terminus and Lys86, Gly87, Ile88 and Val89 at the C terminus are speculated to contribute the hydrophobicity with respect to the physiochemical properties of their side chains (Figure 3). When Lys2, Phe3, Gln4 were deleted from the N terminus, the mutant (*Hp*GroESΔK2F3Q4) exhibited an elution volume of 11.8 mL (Figure 4(d)), corresponding to a molecular mass of ~30 kDa, which likely migrated from a native form of ~100 kDa (Figure 4(b)) to a significantly smaller one, indicating a structural dissociation from a heptamer to a dimer. After the (nearly) full-length but dimerized *Hp*GroES mutant (i.e. *Hp*GroESΔK2F3Q4) was introduced into the urease-postive *E. coli*, the urease activity was determined as ~1.5 μmol min^{-1} mg^{-1} and consequently resulted in an increase of the medium pH to 8.5 (Figure 5(e)), which is comparable to the control level, indicating no significant effect on the urease inactivation. Therefore, the inhibition of urease activity relies on the structural integrity of *Hp*GroES, and furthermore, such an outcome constitutes the evidence of a chaperonin-mediated basis.

3.3 The urease inactivation is also dependent on the metal-binding C terminus

To understand how specific the protein sequence has to be, an alternative version of GroES, *E. coli* GroES (herein named as *Ec*GroES-MBD_0), as well as an MBD-fused mutant (named as *Ec*GroES-MBD_1) have been examined under similar conditions, whose theoretical molecular masses are 10.4 and 14.1 kDa, respectively. As expected, the elution volumes were 10.0 and 10.4 mL for the two proteins (Figure 4(e) and (f)), corresponding to molecular masses of ~90 and ~120 kDa, indicative of a migration as a heptameric complex for both proteins. It is also noticed that the observed molecular masses were apparently larger than the predicted.

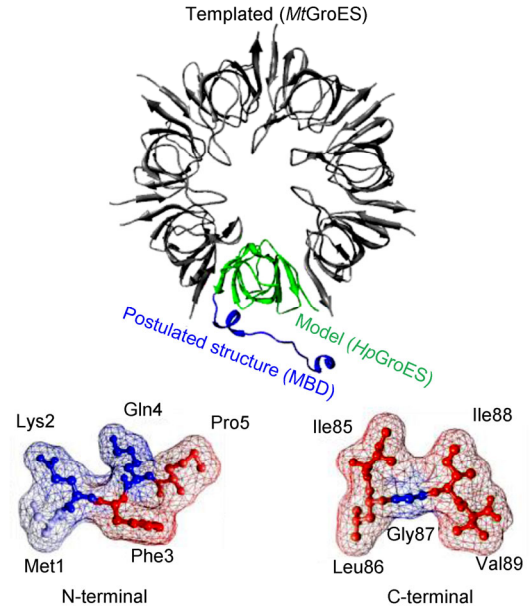

Figure 3 Visual inspection of *Hp*GroES chaperonin. The heptameric structure of *Mycobacterium tuberculosis* GroES (*Mt*GroES, PDB code: 1P3H) with a subunit replaced by a modeled *Hp*GroES monomer. *Mt*GroES is shown in gray, and *Hp*GroES in green. The postulated structure of the MBD is distinguished in blue, with proportional length to the rest of the structure. The two terminal fragments based on the homology model of *Hp*GroES are shown in ball and stick model. Solvent accessible surface of the residues is colored in gradient from red (as hydrophobicity) to blue (as hydrophilicity).

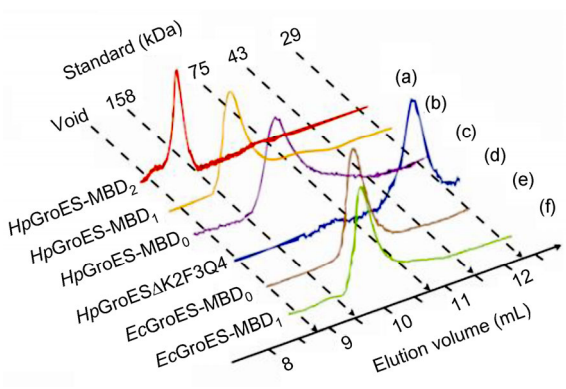

Figure 4 Gel filtration profiles of GroES variants. Proteins in apo-form were subjected to size-exclusive gel filtration chromatography at ambient temperature. The molecular markers were given by standard globular proteins on top of the figure.

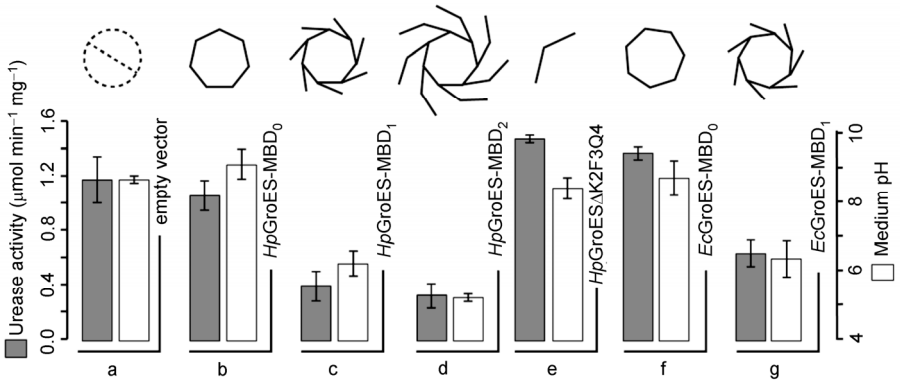

Figure 5 Effects of GroES variants on the rates of urea hydrolysis, which reflects the urease activity, and medium pH. Both indicate the urease activity of the *E. coli* cells harboring urease gene cluster, with or without co-expression of diverse GroES chaperonins. Oligomeric states of the investigated proteins are illustrated on the right side of bars. Each datum was done in quadruplicates, represented as the mean ± the standard deviation.

This may be attributed to the non-globular shape of GroES proteins and the flexible MBD. When co-expressing the wild-type *E. coli* GroES proteins with *H. pylori* urease, the ammonium production was at around 1.3 μmol min^{-1} mg^{-1}, that subsequently let the medium pH rise up to 8.6 (Figure 5(f)). This is similar to the control group, indicative of little effect on the urease activity, which thus excludes the possible interference by the internal presence of *E. coli* GroES. In contrast, in the presence of an MBD-fused derivative (i.e. *Ec*GroES-MBD$_1$), the urease activity was declined to only half of the enzyme activity (~0.6 μmol min^{-1} mg^{-1}) and consequently the medium pH was suppressed to slightly acidic (~6.4) (Figure 5(g)). With reference to the size-exclusive chromatography (Figure 4(e) and (f)), the oligomeric states of the two proteins remained intact, i.e. the native heptameric forms, and therefore the difference in urease activities determined for the *E. coli* GroES variants may not be attributed to a structural abnormality as *Hp*GroESΔK2F3Q4. Taken together, this set of data manifests a weak selectivity for the chaperone region of GroES during the inactivation of urease, as long as the MBD is C-terminally fused to a GroES homolog. In spite, attention should be paid to the fact that a chaperonage-active GroES *per se* is still required since when the MBD was fused to a non-GroES protein (i.e. human glutathione-S-transferase, GST), the chimeric protein was unable to inhibit the urease activity under identical conditions (data not shown).

3.4 *In situ* urease visualization indicated similar urease amounts from the studied samples

It is possible that the changed rate of urea hydrolysis could be caused by the changed expression level of urease rather than enzymatic activity, considering the presence of different GroES variants. To exclude such a possibility, the urease was visualized on native polyacrylamide gel by pH-sensitive dye. According to the result (Figure 6), it appeared that the slight difference among urease bands was far off the proportion to the change of urease activity, so the presumable different amounts of urease should not account for the significant change of urease activity in the studied samples.

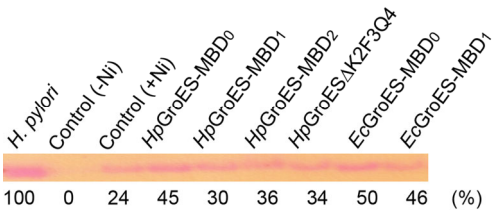

Figure 6 *In situ* visualization of active urease. *H. pylori*, cell extract from the cultivated *H. pylori*; control (-Ni), urease-harboring *E. coli* grown in the absence of nickel; control (+Ni), urease-harboring *E. coli* in the presence of nickel; *Hp*GroES-MBD$_0$, *Hp*GroES-MBD$_1$, *Hp*GroES-MBD$_2$, *Hp*GroESΔK2F3Q4, *Ec*GroES-MBD$_0$ and *Ec*GroES-MBD$_1$: *E. coli* cells with *H. pylori* urease gene cluster and co-transformed GroES variants, grown with nickel supplemented. The amounts of urease were estimated by pixel quantification and shown in relative percent with reference to active urease in *H. pylori* (as 100%) and inactive urease in *E. coli* (as 0%).

3.5 The metal-binding ability is necessary but not the metal-binding capacity in order to inactivate urease

According to the biochemical assays on *E. coli* without any heterologous GroES, urea in the medium was substantially hydrolyzed into ammonia at a rate of ~1.2 μmol min^{-1} mg^{-1}, and thus elevated medium pH from 5.0 to 8.7 (Figure 5(a)), similarly to that expressing the MBD-truncated *Hp*GroES (named as *Hp*GroES-MBD$_0$) (Figure 5(b)). In contrast, the expression of the wild-type *Hp*GroES (i.e. *Hp*GroES-MBD$_1$) exhibited a 3.0-fold inhibition of urease activity to ~0.4 μmol min^{-1} mg^{-1}, resulting in only a slight increase in medium pH to 6.2 (Figure 5(c)). Notwithstanding, compared with *Hp*GroES-MBD$_1$, the MBD-duplicated mutant (i.e. *Hp*GroES-MBD$_2$) contributed slight enhancement to the inhibitory effect, leading to an apparent urease activity at ~0.3 μmol min^{-1} mg^{-1} and keeping the medium pH to maintain 5.0 (Figure 5(d)), although the Ni^{2+} capacity is significantly increased from 2.0 of the wild type to 5.2 of the mutant per monomer (Figure 7). As expected, the MBD-

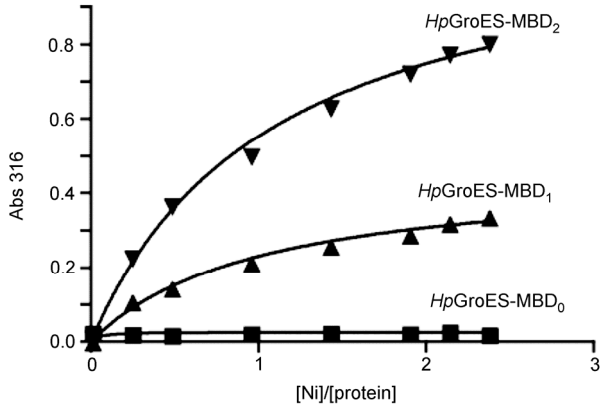

Figure 7 Estimation of the maximal binding ratios (B_{max}) for *Hp*GroES proteins with varying C terminus. The absorption at 316 nm (Abs_{316}) was used to monitor Ni^{2+}-protein interactions by addition of Ni^{2+} (as $NiSO_4$).

truncated mutant showed no detectable binding of Ni^{2+} (Figure 7), so did *Ec*GroES-MBD_0 (data not shown). Note that *Hp*GroES-MBD_1 and -MBD_2 bound 2.0 and 5.2 Ni^{2+} per monomer (R^2 as 0.989 and 0.996), respectively. Unsurprisingly, there was virtually no Ni^{2+} binding to *Hp*GroES-MBD_0, nor *Ec*GroES-MBD_0 (data not shown). As conclusion, the observed result excludes the Ni^{2+} capacity of the MBD as the major cause of the urease inactivation, although the metal-binding ability of the MBD *per se* may indeed play certain functional roles, with respect to the observation of a manganese-increased GroE/S functionality [22].

4 Discussion

A few points can be considered further to interpret our data. First, since *Hp*GroES has been previously determined as a target of immune response, which consequently provides protection against *H. pylori* infection [23], drugs that destroy the chaperonin may contribute to the resistance of the pathogen. Besides, implied by the fact that *Hp*GroES (together with *Hp*GroEL) are induced in *H. pylori* above pH 7, it seems reasonable for the neutrophilic bacterium to utilize the chaperonin under neutral rather than acid physiological conditions that has been ever suggested [12]. Secondly, because the dimeric *Hp*GroES has been detected from *H. pylori*-infected patients [24], *H. pylori* may regulate urease activity simply by switching the oligomeric states of *Hp*GroES between heptamer and dimer. Such an approach is obviously more economic than to degrade either *Hp*GroES or urease, provided that urease inactivation is necessary. Despite the transient oligomers found in GroES folding [25], further study is still required to investigate whether there exists an oligomeric equilibrium of the chaperonin *in vivo*. Thirdly, as the alternative treatment appears effective in *H. pylori* infection by combining bismuth compounds and proton pump inhibitors (PPIs) [26], our findings hint at the possible mechanisms underlying the clinical practice, i.e. bismuth dimerizes *Hp*GroES [13] to unleash urease activity, and meanwhile PPI blocks gastric acid secretion [27] to strengthen the urease-induced alkalinity. Further understanding of the issue may motivate broad trials based on urease inactivation to repel other deadly microbes, as demonstrated for *Mycobacterium tuberculosis* [28].

On the flip side, however, the biological function of *Hp*GroES may be more complicated than expected. Being able to reversibly interact with Ni^{2+} at a physiological concentration, the Ni^{2+}-binding ability of this universal chaperonin should be deductively correlated with the nickel-containing enzymes in *H. pylori*. However, genetic deletion of the MBD-coding sequence led to little influence on urease activity in *H. pylori* [31]. Whereas an early report observed that *Hp*GroES increased urease activity when their genes were co-introduced into *E. coli*, although a nickel-specific transporter (NixA) was not included in the test [12]. The diverse results, including the findings in this work, might be caused by the different selection of cell models. Since the genomics research has implicated a loose restriction of sequence and location specificity for histidine-rich motifs [32], the deletion of one motif might be functionally compensated by the presence of another in a correlated metalloprotein, especially in the original cellular environment (i.e. in *H. pylori*). Notwithstanding, the similar compensation could be hardly accomplished if given a heterogeneous situation where internal urease is inactive (e.g. in *E. coli*), which may exclude the possible interference by the homologous proteins. But strictly speaking, it still remains an open question whether the observed urease inactivation could be possibly attributed to artificial results, due to the study on *H. pylori* proteins in *E. coli* system. Therefore, further study is definitely a must in order to reveal the real scenario regarding this controversy, in particular, direct determination of *in vitro* urease-*Hp*GroES interaction.

Nonetheless, from a practical point of view, the findings herein may not only be helpful for understanding the pathology of *H. pylori*, but also be useful for better design of novel antibiotics. It has been long recognized that chaperones, as well as the related cell stress, hold potential in medicinal applications [29]. Being a uniquely modified ubiquitous chaperone, it has been repetitively evidenced that *Hp*GroES could serve as either a vaccine [23], or a metallodrug target [30]. The broader exploration of its interaction with other proteins, even by artificial means, holds the potential to expand the applications of this unique chaperonin, e.g. to switch ON/OFF status of urease activity simply by metallodrug supplementation or protein expression induction, which could be very useful in the study of nickel trafficking network for urease maturation [2, 33, 34]. Besides, the study on the interactions between nickel and the C terminus of *Hp*GroES also brings up new instance for both histidine-rich sequences [35] and structures [36] of our recent interest.

This work was supported by Research Grants Council of Hong Kong (HKU7042/07P, HKU7049/09P and HKU7046/12P). We thank Drs. D. J. McGee and H. L. Mobley (USA) for providing the urease plasmid (pHP8080), and C. N. Tsang for constructing the expression vectors of EcGroES variants.

1 Covacci A, Telford JL, Del Giudice G, Parsonnet J, Rappuoli R. *Helicobacter pylori* virulence and genetic geography. *Science*, 1999, 284: 1328–1333
2 Carter EL, Flugga N, Boer JL, Mulrooney SB, Hausinger RP. Interplay of metal ions and urease. *Metallomics*, 2009, 1: 207–221
3 Stingl K, Altendorf K, Bakker EP. Acid survival of *Helicobacter pylori*: how does urease activity trigger cytoplasmic pH homeostasis? *Trends Microbiol*, 2002, 10: 70–74
4 Gobert AP, McGee DJ, Akhtar M, Mendz GL, Newton JC, Cheng Y, Mobley HL, Wilson KT. *Helicobacter pylori* arginase inhibits nitric oxide production by eukaryotic cells: a strategy for bacterial survival. *Proc Natl Acad Sci USA*, 2001, 98: 13844–13849
5 Clyne M, Labigne A, Drumm B. *Helicobacter pylori* requires an acidic environment to survive in the presence of urea. *Infect Immun*, 1995, 63: 1669–1673
6 Stingl K, De Reuse H. Staying alive overdosed: how does *Helicobacter pylori* control urease activity? *Int J Med Microbiol*, 2005, 295: 307–315
7 Macario AJ. Heat-shock proteins and molecular chaperones: implications for pathogenesis, diagnostics, and therapeutics. *Int J Clin Lab Res*, 1995, 25: 59–70
8 Tang YC, Chang HC, Roeben A, Wischnewski D, Wischnewski N, Kerner MJ, Hartl FU, Hayer-Hartl M. Structural features of the GroEL-GroES nano-cage required for rapid folding of encapsulated protein. *Cell*, 2006, 125: 903–914
9 Gupta RS. Evolution of the chaperonin families (Hsp60, Hsp10 and Tcp-1) of proteins and the origin of eukaryotic cells. *Mol Microbiol*, 1995, 15: 1–11
10 Saibil H. The lid that shapes the pot: structure and function of the chaperonin groes. *Structure*, 1996, 4: 1–4
11 Gupta RS, Golding GB. Evolution of Hsp70 gene and its implications regarding relationships between archaebacteria, eubacteria, and eukaryotes. *J Mol Evol*, 1993, 37: 573–582
12 Kansau I, Guillain F, Thiberge JM, Labigne A. Nickel binding and immunological properties of the C-terminal domain of the *Helicobacter pylori* groes homologue (HspA). *Mol Microbiol*, 1996, 22: 1013–1023
13 Cun S, Li H, Ge R, Lin MC, Sun H. A histidine-rich and cysteine-rich metal-binding domain at the C terminus of heat shock protein A from *Helicobacter pylori*: implication for nickel homeostasis and bismuth susceptibility. *J Biol Chem*, 2008, 283: 15142–15151
14 Conway de Macario E, Macario AJ. Methanogenic archaea in health and disease: a novel paradigm of microbial pathogenesis. *Int J Med Microbiol*, 2009, 299: 99–108
15 Kamireddi M, Eisenstein E, Reddy P. Stable expression and rapid purification of *Escherichia coli* GroEL and GroES chaperonins. *Protein Expr Purif*, 1997, 11: 47–52
16 Pieper U, Eswar N, Webb BM, Eramian D, Kelly L, Barkan DT, Carter H, Mankoo P, Karchin R, Marti-Renom MA, Davis FP, Sali A. Modbase, a database of annotated comparative protein structure models and associated resources. *Nucleic Acids Res*, 2009, 37: D347–D354
17 McGee DJ, May CA, Garner RM, Himpsl JM, Mobley HL. Isolation of *Helicobacter pylori* genes that modulate urease activity. *J Bacteriol*, 1999, 181: 2477–2484
18 Schneider CA, Rasband WS, Eliceiri KW. NIH image to ImageJ: 25 years of image analysis. *Nat Methods*, 2012, 9: 671–675
19 Bradford MM. A rapid and sensitive method for the quantitation of microgram quantities of protein utilizing the principle of protein-dye binding. *Anal Biochem*, 1976, 72: 248–254
20 Weber F, Keppel F, Georgopoulos C, Hayer-Hartl MK, Hartl FU. The oligomeric structure of GroEL/GroES is required for biologically significant chaperonin function in protein folding. *Nat Struct Biol*, 1998, 5: 977–985
21 Guidry JJ, Shewmaker F, Maskos K, Landry S, Wittung-Stafshede P. Probing the interface in a human co-chaperonin heptamer: Residues disrupting oligomeric unfolded state identified. *BMC Biochem*, 2003, 4: 14
22 Diamant S, Azem A, Weiss C, Goloubinoff P. Increased efficiency of GroE-assisted protein folding by manganese ions. *J Biol Chem*, 1995, 270: 28387–28391
23 Ferrero RL, Thiberge JM, Kansau I, Wuscher N, Huerre M, Labigne A. The GroES homolog of *Helicobacter pylori* confers protective immunity against mucosal infection in mice. *Proc Natl Acad Sci USA*, 1995, 92: 6499–6503
24 Lin YF, Wu MS, Chang CC, Lin SW, Lin JT, Sun YJ, Chen DS, Chow LP. Comparative immunoproteomics of identification and characterization of virulence factors from *Helicobacter pylori* related to gastric cancer. *Mol Cell Proteomics*, 2006, 5: 1484–1496
25 Perham M, Chen M, Ma J, Wittung-Stafshede P. Unfolding of heptameric co-chaperonin protein follows "fly casting" mechanism: observation of transient nonnative heptamer. *J Am Chem Soc*, 2005, 127: 16402–16403
26 Axon A. Treatment of *Helicobacter pylori*: Where are we now? What are the key questions? *Eur J Gastroen Hepat*, 1999, 11 Suppl 2(S3-7); discussion S23–24
27 Sachs G. Proton pump inhibitors and acid-related diseases. *Pharmacotherapy*, 1997, 17: 22–37
28 Kaplan G. Rational vaccine development: a new trend in tuberculosis control. *N Engl J Med*, 2005, 353: 1624–1625
29 Voellmy R. Review of patents in the cell stress and chaperone field. *Cell Stress Chaperones*, 1996, 1: 29–32
30 Cun S, Sun H. A zinc-binding site by negative selection induces metallodrug susceptibility in an essential chaperonin. *Proc Natl Acad Sci USA*, 2010, 107: 4943–4948
31 Schauer K, Muller C, Carrière M, Labigne A, Cavazza C, De Reuse H. The *Helicobacter pylori* GroES co-chaperonine HspA functions as a specialized nickel-chaperone and sequestration protein through its unique C-terminal extension. *J Bacteriol*, 2010, 192: 1231–1237
32 Haas CE, Rodionov DA, Kropat J, Malasarn D, Merchant SS, de Crécy-Lagard V. A subset of the diverse Cog0523 family of putative metal chaperones is linked to zinc homeostasis in all kingdoms of life. *BMC Genomics*, 2009, 10: 470
33 Zambelli B, Musiani F, Benini S, Ciurli S. Chemistry of Ni^{2+} in urease: sensing, trafficking, and catalysis. *Acc Chem Res*, 2011, 44: 520–530
34 Mobley HL, Island MD, Hausinger RP. Molecular biology of microbial ureases. *Microbiol Rev*, 1995, 59: 451–480
35 Cheng T, Xia W, Wang P, Huang F, Wang J, Sun H. Histidine-rich proteins in prokaryotes: metal homeostasis and environmental habitat-related occurrence. *Metallomics*, 2013, 5: 1423–1429
36 Cun S, Lai YT, Chang YY, Sun H. Structure-oriented bioinformatic approach exploring histidine-rich clusters in proteins. *Metallomics*, 2013, 5: 904–912